



City Research Online

City, University of London Institutional Repository

Citation: Chen, X., Zhang, Q., Ming, Y., Fu, F. & Rong, H. (2023). A Numerical study for Chloride Migration in Concrete Under Electrochemical Repair Process. Proceedings of the Institution of Civil Engineers: Structures and Buildings, 176(7), pp. 556-564. doi: 10.1680/jstbu.21.00049

This is the accepted version of the paper.

This version of the publication may differ from the final published version.

Permanent repository link: <https://openaccess.city.ac.uk/id/eprint/26655/>

Link to published version: <https://doi.org/10.1680/jstbu.21.00049>

Copyright: City Research Online aims to make research outputs of City, University of London available to a wider audience. Copyright and Moral Rights remain with the author(s) and/or copyright holders. URLs from City Research Online may be freely distributed and linked to.

Reuse: Copies of full items can be used for personal research or study, educational, or not-for-profit purposes without prior permission or charge. Provided that the authors, title and full bibliographic details are credited, a hyperlink and/or URL is given for the original metadata page and the content is not changed in any way.

City Research Online:

<http://openaccess.city.ac.uk/>

publications@city.ac.uk

36 **1 Introduction**

37 In offshore engineering structures, chloride is one of the main factors causing reinforcing bar
38 corrosion (Arya, Vassie and Bioubakhsh, 2014; Kumar, Kumar and Kujur, 2019; Wang, Gong and
39 Wu, 2019). Electrochemical repair is one of effective methods to remove chloride in concrete and
40 improve the durability of offshore engineering structures (Xia *et al.*, 2019). Electrochemical
41 chloride removal (ECR) technique refers to the formation of potential difference between
42 reinforcing bar (*i.e.*, cathode) and external electrolyte (*i.e.*, anode). Under the action of potential
43 difference, chloride in concrete moves from low potential to high potential, so as to remove chloride
44 in concrete (Shi *et al.*, 2012; Xia *et al.*, 2019; Xu and Li, 2019a).

45 ECR technique has been favored by many research scholars since the experimental
46 investigation work was carried out in the 1970s (Garcés, Sánchez De Rojas and Climent, 2006;
47 Miranda *et al.*, 2007; Sánchez and Alonso, 2011). Mao *et al.*(Mao *et al.*, 2015) studied the effect of
48 external electric field on chloride removal in sea sand concrete. And the research indicated that
49 external electric field could effectively remove chloride in sea sand concrete, and the durability of
50 sea sand concrete could be greatly improved by migrating corrosion inhibitor into reinforcing bar
51 surface. The study of Zhou *et al.* (Zhou *et al.*, 2020) manifested that external electric field could
52 effectively remove chloride in concrete, but it also led to the migration and aggregation of a large
53 number of K^+ and Na^+ ions to the arear near the reinforcing bar. Saraswathy *et al.* (Saraswathy, H.-
54 S. Lee, *et al.*, 2018) investigated the effect of different anode types on chloride removal efficiency.
55 Xia, J. *et al.* (Xia, Q. Liu, *et al.*, 2018) discussed the effect of ambient temperature on ECR efficiency.
56 The study displayed that the total efficiency was doubled as the temperature increased from 0°C to
57 20°C, and it was improved by 13% as the temperature reached 50°C, indicating that temperature
58 rise was an effective method of improving ECR efficiency. However, concrete is a heterogenous
59 material with complex microstructure. Due to the interaction between different factors, it's hard to
60 determine the individual effects of various factors through experiments. Comparatively speaking,
61 numerical models have great advantages in providing detailed information and studying research
62 parameters.

63 With the progress of computer science and technology and the development of finite element
64 numerical method, especially for complicated multi-field coupling problems, numerical simulation
65 technique has been extensively applied. In the existing ECR numerical models (Li and Page, 1998;
66 Toumi, François and Alvarado, 2007; Xia, Q. feng Liu, *et al.*, 2018), it's assumed that concrete was
67 isotropic material, and Nernst-Planck equation was used to simulate the chloride removal process
68 of reinforced concrete under the action of potential. The effects of treatment time, current density,
69 binding effect, additive, and temperature on ECR efficiency were studied. Li, *et al.* (Li and Page,
70 2000) established a numerical electrochemical chloride removal model by using Nernst-Planck

71 equation, and solved the Nernst-Planck equation by employed finite element method. And the
72 effects of external current density, treatment time, ion coefficient, ion binding, boundary condition
73 and medium porosity on chloride extraction efficiency were studied. Xu, Jun et al. (Xu and Li,
74 2019b) established the fitting formulas of chloride removal efficiency of unilateral-anode concrete
75 with current density and treatment time. Liu, Q., *et al.* (Liu *et al.*, 2015) discussed the effects of
76 aggregate shape, boundary conditions and double electrode layers on ECR efficiency and ion
77 concentration distribution.

78 Many researchers have conducted a large quantity of fundamental studies on ECR, providing
79 a theoretical and experimental basis for follow-up ECR researches (Liu *et al.*, 2014). However, all
80 of the abovementioned researches are based on uniform chloride distribution in concrete. While in
81 practical engineering, the distribution of chloride in concrete is nonuniform. The concentration of
82 chloride ions near the erosion surface is higher, while the chloride concentration away from erosion
83 surface is lower. In this paper, the distribution of free chloride in practical engineering is simulated
84 through two stages, *i.e.*, the diffusion of free chloride and electric migration. The external electric
85 field is applied to remove chloride ions diffused into the concrete. The numerical electrochemical
86 repair model with diffusion-electric migration is established, and the chloride distribution laws in
87 the concrete are investigated.

88 **2. Theoretical background**

89 **2.1 Chloride diffusion**

90 In offshore engineering structures, chloride ions in the environment diffuse into the concrete
91 due to the chloride concentration difference (Chen *et al.*, 2020, 2021). The studies of many
92 researchers indicates that chloride diffusion conforms to Fick's second Law, and the chloride
93 diffusion equation in the concrete is as follow (DHIR, JONES and MCCARTHY, 1993; Jin *et al.*,
94 2015; Zhu and Zi, 2017; Mazer, Lima and Medeiros-Junior, 2018; Wang *et al.*, 2018):

$$95 \quad \frac{\partial C}{\partial t} = \nabla(D_{cl}\nabla C) \quad (1)$$

96 where t is the erosion time of chloride, C is the chloride concentration (by weight of concrete, %),
97 and D_{cl} is chloride diffusion coefficient, respectively. It can be seen from Eq. (1) that D_{cl} is a
98 decisive factor for chloride concentration in concrete. The chloride ion diffusion coefficient not only
99 relates to the concrete itself (such as concrete type, pore structure, water-binder ratio, hydration
100 degree and so on), but also relates to the external environment, such as temperature (Bažant and
101 Najjar, 1972), humidity (Muthulingam and Rao, 2014), maintenance age (Martín-Pérez,
102 Pantazopoulou and Thomas, 2001) and other factors. In this paper, only the effects of water-binder
103 ratio, temperature, humidity, and age are considered in the chloride diffusion coefficient. And the

104 chloride diffusion coefficient can be expressed as (Jin *et al.*, 2015; Wang *et al.*, 2018; Chen *et al.*,
105 2020):

$$106 \quad D_c = \underbrace{\frac{2 \times \varphi_p^{2.75} D_p}{\varphi_p^{1.75} (3 - \varphi_p) + n(1 - \varphi_p)^{2.75}}}_{\text{Water-cement ratio}} \cdot \underbrace{\exp\left[\frac{U_c}{R} \left(\frac{1}{T_{ref}} - \frac{1}{T}\right)\right]}_{\text{Temperature}} \cdot \underbrace{\left[1 + \frac{(1-h)^4}{(1-h_c)^4}\right]^{-1}}_{\text{Humidity}} \cdot \underbrace{\left(\frac{t_{ref}}{t}\right)^m}_{\text{Curing age}} \quad (2)$$

107 where U_c is the chloride diffusion activation energy (44.6KJ/mol), t_{ref} is the reference exposure
108 time (28 d), t is the chloride ion erosion time (s), T is the ambient temperature (K), R is the gas
109 constant (8.314 J/K·mol), T_{ref} is the reference temperature (298 K), h is the humidity and h_c
110 the critical humidity (0.75). D_p is the chloride diffusion coefficient in water ($1.07 \times 10^{-10} \text{ m}^2/\text{s}$), n
111 is the empirical parameter (14.44) (Du, Jin and Ma, 2014), m is the time attenuation index. And φ_p
112 is the porosity of cement paste, which can be expressed as (Sun *et al.*, 2011)

$$113 \quad \varphi_p = \frac{wc - 0.17\alpha}{wc + 0.32} \quad (3)$$

114 where α is the degree of hydration of cement paste, and wc is the ratio of water to binder.

115 2.2 Electrochemical migration

116 As is known, the concrete pore solution contains various ions. Under the action of external
117 electric field, positively charged ions move towards low potential, and negatively charged ones
118 move towards high potential (Liu *et al.*, 2015; Chen *et al.*, 2021). Assuming that the concrete pore
119 solution is diluted solution and the internal ions do not react with each other, the ion concentration
120 in the concrete under the action of electric field can be calculated according to Nernst-Planck
121 equation. The material equilibrium and ion transfer are defined by combing electric neutrality
122 condition (Xu and Li, 2019a; Chen *et al.*, 2021; Fang *et al.*, 2021).

$$123 \quad \frac{\partial C_i}{\partial t} = \nabla \cdot \left(D_i \nabla C_i + z_i D_i \left(\frac{F}{RT} \nabla \phi \right) C_i \right) \quad (4)$$

$$124 \quad I = F \sum_{i=1}^n z_i \left(-D_i \nabla C_i - z_i D_i \left(\frac{F}{RT} \nabla \phi \right) C_i \right) \quad (5)$$

$$125 \quad \sum_{i=1}^n z_i C_i = 0 \quad (6)$$

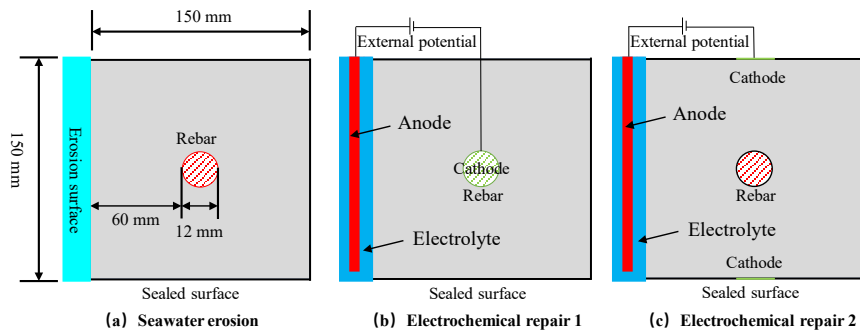
126 where C_i , D_i , and z_i represent the concentration, diffusion coefficient and charge number of the
127 i -th ionic species in concrete, respectively. $F=9.648 \times 10^4 \text{ C} \cdot \text{mol}^{-1}$ is the Faraday constant, ϕ is the
128 electric potential.

129 3 Numerical simulations

130 During concrete pouring process in the actual projects, the concrete pore solution contains
131 various ions, mainly including K^+ , Na^+ , Ca^{2+} and OH^- ions. These ions are formed during the pouring

132 process and are uniform distribution in the concrete. The chloride content is very small and can be
 133 ignored during the pouring process. However, during the service process of concrete, chloride ions
 134 in the environment gradually penetrated concrete. The free chloride diffusion process is simulated
 135 by Eq. (1), in which the external electric field is not applied. After chloride diffusion for a certain
 136 time, an external electric field is applied to remove chloride ions from concrete. The ion
 137 concentration distributions at different time are calculated by Eqs. (4) ~ (6).

138 Wu *et al.* (Wu, Li and Yu, 2017) performed on-situ chloride sampling and testing at 13# wharf
 139 of Fangcheng Port, Beibu Gulf in Guangxi Province. The results showed that the chloride
 140 concentration in the outmost layer was about 0.67%, which was converted into Molar concentration
 141 of 471.8 mol/m³. Therefore, the boundary concentration of chloride ions on the erosion surface is
 142 taken as 471.8 mol/m³ in this paper. In the 10th year after chloride ion free erosion, electrochemical
 143 repair is started. The chloride concentration in the concrete is Cl_{10} , and the chloride diffusion
 144 coefficient is D_{cl10} . The boundary concentrations and diffusion coefficients of other ions can refer
 145 to references shown in **Tab. 1**. **Fig. 1** is the schematic diagram of chloride attack on concrete and
 146 electrochemical repair. The diameter of the reinforcing bar is 12 mm, the thickness of the concrete
 147 cover is 60 mm, and the geometric dimension of concrete section is 150 mm x 150 mm, respectively.



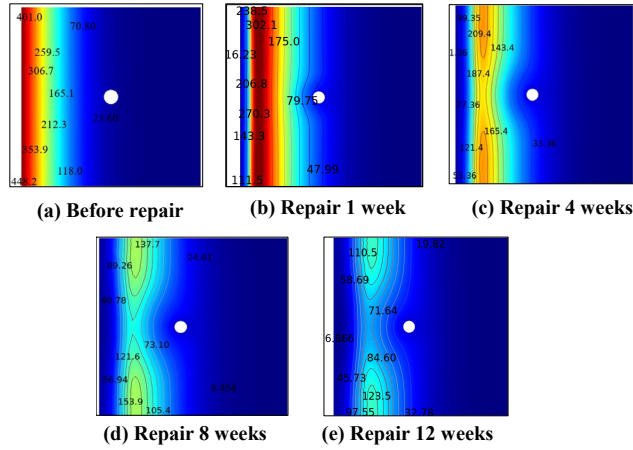
148
149 **Fig. 1.** Numerical simulation diagram.

150 **Table 1** Boundary conditions, initial values, and diffusion coefficients of various ion (Wang, Li and Page, 2001;
 151 Liu *et al.*, 2012; Xia *et al.*, 2020).

Field variables	Position	K ⁺	Na ⁺	Ca ²⁺	OH ⁻	Cl ⁻
Charge number	--	+1	+1	+2	-1	-1
Boundary concentration (mol/m ³)	Anode	5	5	25.2	12.6	10
Flux boundary condition	Sealing	0	0	0	0	0
Initial concentration (mol/m ³)	Internal	100	Cl_{10}	Cl_{10}	100	0

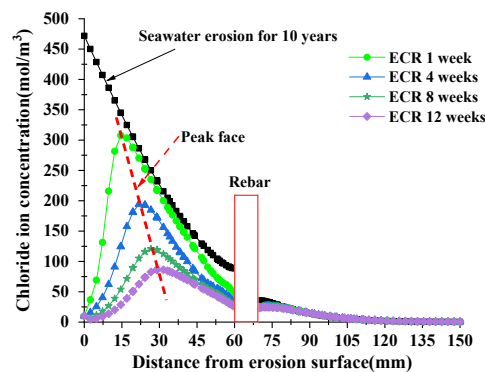
152 **4. Result analysis and discussion**

153 **4.1 Chloride concentration distribution**



154 **Fig. 2.** Chloride concentration distribution cloud map.

156 **Fig. 2a** shows the free chloride concentration distribution in the 10th year of chloride diffusion.
 157 In the electrochemical repair process, the reinforcement bar is used as cathode, as shown in **Fig. 1b**.
 158 And the applied electric potential is 12 V. Additionally, the distributions of free chloride with
 159 different electrochemical repair time are shown in **Fig. 2b-e**. It can be seen from **Fig. 2a-e** that under
 160 the action of external electric field, chloride ions are removed from concrete. The chloride
 161 distributions in the concrete after electrochemical repair (as shown in **Fig. 2b-e**) are very different
 162 from that in the free diffusion stage (as shown in **Fig. 2a**). Compared with that before
 163 electrochemical repair (as shown in **Fig. 2a**), the chloride concentrations near the erosion surface
 164 (as shown in **Fig. 2b-e**) are lower after electrochemical repair. With the increase of erosion depth,
 165 chloride concentration first gradually increases and then decreases. Chloride ions migrate outward
 166 rapidly due to the applied low electric field around the reinforcing bar. With the increase of
 167 electrochemical repair time, the total chloride content in concrete gradually decreases, indicating
 168 that electrochemical repair is an effective method to remove chloride ions from concrete.



170

Fig. 3. Chloride concentration along the depth distribution curve

171

Fig. 3 shows the chloride concentration distribution curves in concrete at 1 week, 4 weeks, 8 weeks, and 12 weeks of electrochemical repair. It is obvious from **Fig. 3** that the peak value of chloride concentration in concrete appear at 15 mm~30 mm away from the erosion surface. With the increase of the electrochemical repair time, the peak concentration of chloride gradually decreases and gradually moves towards the interior of concrete, which indicates that chloride ions in concrete are continuously remove from concrete under the action of external electric field. After 12 weeks of electrochemical repair, the peak value of chloride concentration decreases to 86.55 mol/m³. Additionally, the chloride concentration near the erosion surface changes obviously, while the change of chloride concentration on the other side of erosion surface is not obvious. Similar conclusions were also found in the study of Chen *et al* (Chen *et al.*, 2021).

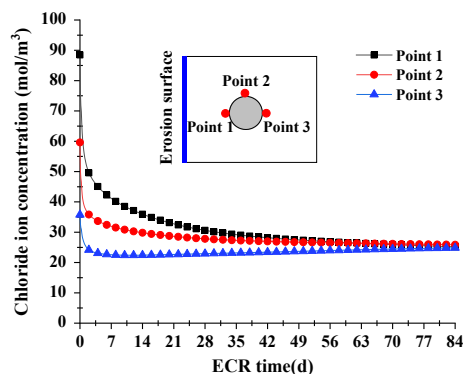
181

4.2 Chloride concentration on reinforcing bar surface

182

For reinforced concrete, the chloride concentration on the reinforcing bar surface is one of critical factors influencing corrosion of reinforcing bar. The chloride concentration on the reinforcing bar surface under the action of external electric field will be analyzed in this section. It should be noted that the position and applied potential of the cathode are the same as those in Section 4.1. *i.e.*, the reinforcing bar is used as cathode and the applied electric potential is 12 V. **Fig. 4** shows the chloride concentration curves at three different points on the reinforcing bar surface. It is apparent from **Fig. 4** that the chloride concentrations at three positions decrease with the increase of electrochemical repair time. Moreover, in the first 14 days (14 d) of electrochemical repair, the chloride concentrations decrease sharply and then tended to be stable (about 24 mol/m³). This indicates that the electrochemical repair efficiency cannot be improved by prolonging the repair time when the electrochemical repaired has been carried out for a certain time.

192



193

Fig. 4. Chloride concentration curves on the reinforcing bar surface.

194

195

4.3 ECR efficiency

196

Chloride diffusion is a very slow process, the total chloride content in the concrete has a great influence on the redistribution of chloride after the ECR. Therefore, the total chloride reduction rate

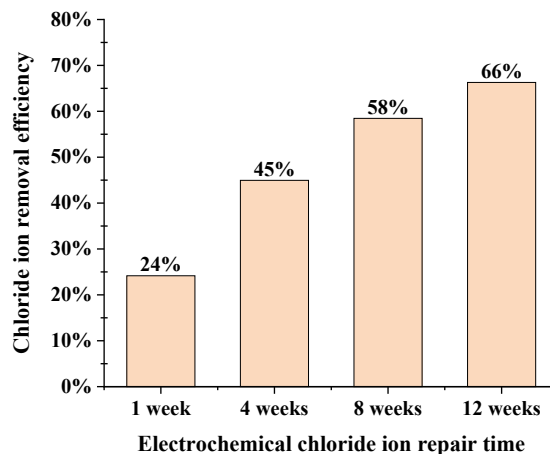
197

198 in concrete is employed in this paper as an evaluation index measuring the repair effect. The
199 calculation formula is as below:

$$200 \quad P = \frac{M_0 - M_t}{M_0} \times 100\% \quad (7)$$

201 where P is the chloride ion reduction rate (%), M_0 is the total amount of initial chloride ion in
202 concrete (mol), M_t is the total concentration of chloride ion in concrete at the time of
203 electrochemical repair (mol).

204 The reinforcing bar is used as cathode and the applied electric potential is 12 V **Fig. 5** shows
205 the histogram of chloride removal rate in concrete at different repair time. It is obvious from **Fig. 5**.
206 that at 1 week, 4 weeks, 8 weeks and 12 weeks of the electrochemical repair, the chloride removal
207 rates are 24%, 45%, 58% and 66%, respectively. This indicates that the electrochemical repair could
208 effectively remove chloride ions in concrete. Meanwhile, with the increase of repair time, the
209 increase amplitude of chloride removal rate gradually decreases. Similar phenomenon has also been
210 found by Saraswathy *et al.* (Saraswathy *et al.* 2017) and Chen *et al.* (Chen *et al.*, 2021).



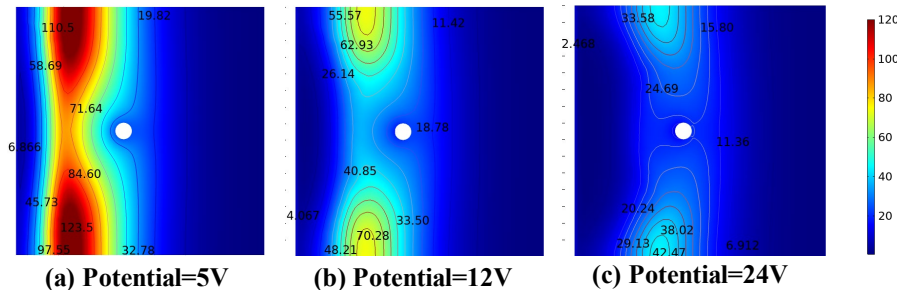
211
212

Fig. 5. ECR efficiency at different repair times.

213 4.4 Effect of different potentials on ECR

214 According to formula (4), the potential gradient is the main driving force for chloride migration.
215 Therefore, the potential difference between anode and cathode plays a very important role in
216 chloride removal rate. **Fig. 6a-c** shows the distributions of chloride concentration at 12 weeks of the
217 electrochemical repair under potentials of 5 V, 12 V and 24 V, respectively. It can be seen from **Fig.**
218 **6a-c** that the chloride concentration in concrete gradually decreases with the increase of potential.
219 For different potentials, the overall chloride concentration are different, while the chloride
220 distribution trend in concrete doesn't changed significantly. It is obvious from that **Fig. 6a-c** two
221 chloride concentration peak points are formed on the side near the erosion surface. Through

222 comparing **Fig. 6a, b** and **c**, it is apparent that the chloride concentration difference between **Fig. 6a**
 223 and **b** is very large, while the chloride concentration difference between **Fig. 6b** and **c** is relatively
 224 small. This indicates that as the potential increase, the influence of potential on chloride
 225 concentration distribution decreases.

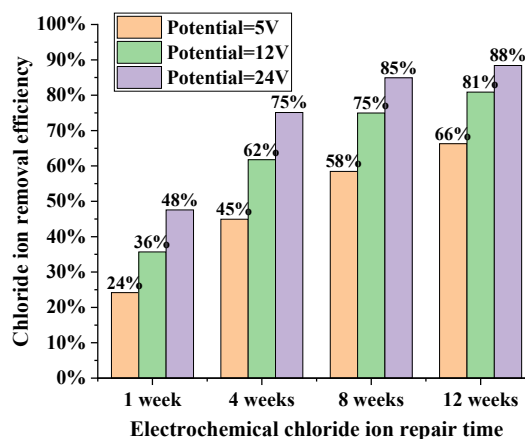


226

227

Fig. 6. Cloud images of different potential potentials.

228 **Fig. 7** shows the chloride removal rate histograms at 1 week, 4 weeks, 8 weeks, and 12 weeks
 229 of electrochemical repair under different potentials. It can be seen from **Fig. 7** that increasing
 230 potential can effectively improve the chloride removal rate. However, too high potential may cause
 231 hydrogen evolution reaction on the reinforcing bar surface and make the reinforcing bar more fragile
 232 (Mao *et al.*, 2019; Chen *et al.*, 2021). At 12 weeks of the electrochemical repair, the chloride removal
 233 rates under external potentials of 5 V, 12 V and 24 V are 66%, 81% and 88%, respectively.,
 234 respectively. Compared with the electrochemical repair time of 8 weeks, the chloride removal rates
 235 under external potentials of 5 V, 12 V and 24 V at the electrochemical repair time of 12 weeks
 236 increase by 8%, 6% and 3%, respectively. While compared with the electrochemical repair time of
 237 4 weeks, the chloride removal rates under external potentials of 5 V, 12 V and 24 V at the
 238 electrochemical repair time of 8 weeks increase by 3%, 13% and 10%, respectively. These results
 239 indicate that the increase of ECR efficiency decreases gradually with the increase of electrochemical
 240 repair time. The chloride migration is mainly driven by electric migration in the early stage of
 241 electrochemical repair, while it is mainly driven by the concentration difference in later stage of
 242 electrochemical repair.



243

244

Fig. 7. ECR repair efficiency with different potentials.

245

4.5 Effect of cathode location on ECR

246

247

248

249

250

251

252

253

254

255

256

257

258

259

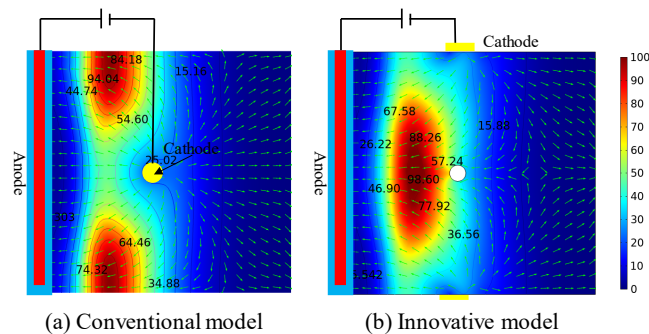
260

261

262

263

According to the above analysis, the electrochemical repair can effectively remove chloride ions in concrete. However, many studies show that ECR will not only eliminate harmful chloride ions, but also have adverse effects on reinforced concrete structure, such as reducing the bonding strength between reinforcing bar and concrete (Nguyen *et al.*, 2021), making the reinforcing bar more fragile (Saraswathy, H. S. Lee, *et al.*, 2018). Meanwhile, Na^+ and K^+ ions in the concrete solution will also aggregate near the reinforcing bar, causing concrete ASR harm. In this section, the chloride distributions in concrete and the ECR efficiency are analyzed when the reinforcing bar is used as cathode and both sides of concrete are used as cathodes. **Fig. 8a-b** show the chloride distributions in concrete at 8 weeks of electrochemical repair. It is apparent from **Fig. 8a-b** that there is great difference in the chloride distributions in concrete with these two cases. Generally, the reinforcing bar is taken as cathode, as is shown in **Fig. 8a**. And the chloride ion concentration near the reinforcement is the lowest, and two peaks of chloride ion concentration are formed in the concrete. When both sides of concrete are used as cathodes, chloride ions move from both sides of the concrete (*i.e.*, cathodes) to the erosion surface (*i.e.*, anode), as is shown in **Fig. 8b**. This results in the lowest chloride concentration on both sides of the concrete (*i.e.*, cathodes) and the highest chloride concentration near the surface of the reinforcement, as is shown in **Fig. 8b**. And a chloride ion concentration peak appears near the reinforcement surface in concrete. Moreover, by comparing **Fig. 8a** and **b**, the peak values of the two cases are almost the same, *i.e.*, about 100 mol/m^3 .



264

265

266

267

Fig. 8. Chloride distributions in concrete with different cathode positions at 8 weeks of electrochemical repair. (a) Reinforcing bar is used as cathode, and (b) both sides of concrete are used cathodes.

268

269

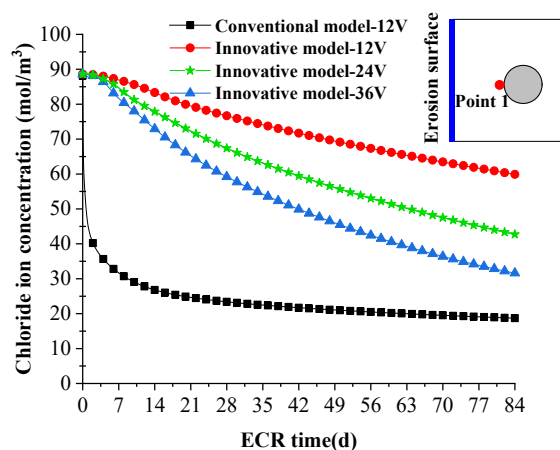
270

271

272

Fig. 9 shows the distributions of chloride ion concentration on the surface of reinforcement with erosion time when reinforcement is used as cathode and both sides of concrete are used as cathode, respectively. It can be seen from **Fig. 9** that under the same external potential of 12 V, the chloride concentration on the reinforcing bar surface in the model with cathodes on both sides of concrete (red dot curve) is much higher than that with cathode on the reinforcing bar (black square

273 curve). Moreover, in the model with reinforcing bar as cathode, the chloride concentration on the
 274 surface of reinforcing bar (black square curve) decreases rapidly and tends to be stable after 14 d of
 275 electrochemical repair. However, for the model with both sides of concrete as cathodes, the chloride
 276 concentration (red dot curve) decreases slowly with electrochemical repair time. Additionally, the
 277 chloride concentration curves with both sides of concrete as cathodes under external potentials of
 278 12 V, 24 V and 36 V are also depicted in **Fig. 9**. It is obvious from **Fig. 9** that the chloride
 279 concentration on the reinforcing bar surface can be effectively reduced by increasing the external
 280 potential. However, the overall electrochemical repair effect in the model with cathodes on both
 281 sides of concrete is still worse than that in the model with reinforcing bar served as cathode.
 282 Nevertheless, from the curve declining trend analysis, the model in which the two sides of concrete
 283 served as the cathode can achieve better chloride removal effect with the increase of electrochemical
 284 repair time.



285
 286 **Fig. 9.** Chloride ion concentration curves on the surface of steel bars for different repair models.

287 **5 Conclusions**

288 In this paper, a numerical chloride migration-diffusion model is established by Nernst-Planck
 289 equation to simulate the chloride erosion process in the external environment and the
 290 electrochemical repair process. Based on a systematic study, the following conclusions can be drawn:

291 (1) Electrochemical repair changes the chloride distribution in concrete. After chloride ions in
 292 the external environment diffuse into the concrete, the chloride ions in the concrete can be
 293 effectively removed by electrochemical repair. After electrochemical repair, the chloride
 294 concentration peak appears at 15 mm ~ 30 mm away from the erosion surface. With the increase of
 295 electrochemical repair time, the peak value of chloride concentrate gradually decreases, and the
 296 peak of chloride concentrate moves toward the interior of concrete.

297 (2) Electrochemical repair can rapidly reduce the chloride concentration on the reinforcing bar
 298 surface. The chloride concentration on the reinforcing bar surface decreases sharply in the beginning
 299 of electrochemical repair and tends to be stable after 14 d of electrochemical repair. Furthermore,
 300 with the increase of external potential, the stabilization time is shortened.

301 (3) Electrochemical repair can effectively reduce the chloride concentration in concrete. When
302 the ratio of chloride ion removal in concrete to the total amount of initial chloride ion is used to
303 measure the ECR efficiency, the ECR efficiency can reach more than 60% after 12 weeks of
304 electrochemical repair. Moreover, the ECR efficiency increases with the increase of external
305 potential.

306 (4) When the cathodes are set on both sides of concrete, the ECR efficiency can be improved
307 by increasing the external potential and lengthening the repair time. From a comparison between
308 the situation with cathodes on both sides of concrete and that with cathode on the reinforcing bar
309 surface, it can be found that there is a great difference in chloride concentration after the
310 electrochemical repair. Moreover, the decreasing curves of chloride concentration on the surface of
311 reinforcement is also different. However, the ECR efficiency with cathodes on both sides of concrete
312 can be improved by prolonging the repair time and increasing the external potential.

313

314 **Author Contributions:**

315 **Xuandong Chen:** Conceptualization, Methodology, Writing- Original draft preparation, Software,
316 Investigation. **Qing Zhang:** Writing-reviewing and Editing, Methodology, conceptualization,
317 Supervision. **Feng Fu:** Data curation, Writing- Reviewing and Editing. **Yang Ming:** Software, Data
318 curation. **Hua Rong:** Methodology, Software, Conceptualization.

319

320 **Acknowledgements:**

321 The present research was financially supported by the Natural Science Foundation of China (Nos.
322 11932006, U1934206, 12002118 , 51968013), National Key Research & Development Plan of
323 China (No. 2018YFC0406703), Guangxi Universities Scientific Research Project (No.
324 2020KY06029), Guangxi Key Laboratory of New Energy and Building Energy Saving Foundation
325 (No. 19-J-21-30), and the Fundamental Research Funds for the Central Universities (Nos.
326 B200202231, B210201031).

327 **Conflicts of Interest:** The authors declare no conflict of interest.

328

329 **References**

- 330 Arya, C., Vassie, P. and Bioubakhsh, S. (2014) 'Chloride penetration in concrete subject to wet-dry
331 cycling: influence of pore structure', *Proceedings of the Institution of Civil Engineers - Structures and*
332 *Buildings*, 167(6), pp. 343–354. doi: 10.1680/stbu.12.00067.
- 333 Bažant, Z. P. and Najjar, L. J. (1972) 'Nonlinear water diffusion in nonsaturated concrete', *Matériaux*

334 *et Constructions*, 5(1), pp. 3–20. doi: 10.1007/BF02479073.

335 Chen, X. *et al.* (2020) ‘A multi-phase mesoscopic simulation model for the diffusion of chloride in
336 concrete under freeze–thaw cycles’, *Construction and Building Materials*, 265, p. 120223. doi:
337 10.1016/j.conbuildmat.2020.120223.

338 Chen, X. *et al.* (2021) ‘A multi-phase mesoscopic simulation model for the long-term chloride ingress
339 and electrochemical chloride extraction’, *Construction and Building Materials*, 270, p. 121826. doi:
340 10.1016/j.conbuildmat.2020.121826.

341 DHIR, R. K., JONES, M. R. and MCCARTHY, M. J. (1993) ‘PFA CONCRETE: CHLORIDE
342 INGRESS AND CORROSION IN CARBONATED COVER.’, *Proceedings of the Institution of Civil
343 Engineers - Structures and Buildings*, 99(2), pp. 167–172. doi: 10.1680/istbu.1993.23375.

344 Du, X., Jin, L. and Ma, G. (2014) ‘A meso-scale numerical method for the simulation of chloride
345 diffusivity in concrete’, *Finite Elements in Analysis and Design*, 85, pp. 87–100. doi:
346 10.1016/j.finel.2014.03.002.

347 Fang, Y. *et al.* (2021) ‘Investigation of electrochemical chloride removal from concrete using direct
348 and pulse current’, *Construction and Building Materials*, 270, p. 121434. doi:
349 10.1016/j.conbuildmat.2020.121434.

350 Garcés, P., Sánchez De Rojas, M. J. and Climent, M. A. (2006) ‘Effect of the reinforcement bar
351 arrangement on the efficiency of electrochemical chloride removal technique applied to reinforced
352 concrete structures’, *Corrosion Science*, 48(3), pp. 531–545. doi: 10.1016/j.corsci.2005.02.010.

353 Jin, L. *et al.* (2015) ‘Multi-scale analytical theory of the diffusivity of concrete subjected to mechanical
354 stress’, *Construction and Building Materials*, 95, pp. 171–185. doi:
355 10.1016/j.conbuildmat.2015.07.123.

356 Kumar, S., Kumar, A. and Kujur, J. (2019) ‘Influence of nanosilica on mechanical and durability
357 properties of concrete’, *Proceedings of the Institution of Civil Engineers - Structures and Buildings*,
358 172(11), pp. 781–788. doi: 10.1680/jstbu.18.00080.

359 Li, L. Y. and Page, C. L. (1998) ‘Modelling of electrochemical chloride extraction from concrete:
360 Influence of ionic activity coefficients’, *Computational Materials Science*, 9(3–4), pp. 303–308. doi:
361 10.1016/s0927-0256(97)00152-3.

362 Li, L. Y. and Page, C. L. (2000) ‘Finite element modelling of chloride removal from concrete by an
363 electrochemical method’, *Corrosion Science*, 42(12), pp. 2145–2165. doi: 10.1016/S0010-

364 938X(00)00044-5.

365 Liu, Q. *et al.* (2015) 'A numerical study on chloride migration in cracked concrete using multi-

366 component ionic transport models', *Computational Materials Science*, 99, pp. 396–416. doi:

367 10.1016/j.commatsci.2015.01.013.

368 Liu, Q. F. *et al.* (2014) 'Three-phase modelling of electrochemical chloride removal from corroded

369 steel-reinforced concrete', *Construction and Building Materials*, 70, pp. 410–427. doi:

370 10.1016/j.conbuildmat.2014.08.003.

371 Liu, Q. feng *et al.* (2012) 'Multi-phase modelling of ionic transport in concrete when subjected to an

372 externally applied electric field', *Engineering Structures*, 42, pp. 201–213. doi:

373 10.1016/j.engstruct.2012.04.021.

374 Mao, J. *et al.* (2015) 'Technology for Enhancing Durability of Structures of Sea-sand Concrete and Its

375 Application', *Journal of Chinese Society for Corrosion and Protection*, 35, pp. 564–570.

376 Mao, J. *et al.* (2019) 'Hydrogen embrittlement risk control of prestressed tendons during

377 electrochemical rehabilitation based on bidirectional electro-migration', *Construction and Building*

378 *Materials*, 213, pp. 582–591. doi: 10.1016/j.conbuildmat.2019.04.008.

379 Martín-Pérez, B., Pantazopoulou, S. J. and Thomas, M. D. A. (2001) 'Numerical solution of mass

380 transport equations in concrete structures', *Computers & Structures*, 79(13), pp. 1251–1264. doi:

381 10.1016/S0045-7949(01)00018-9.

382 Mazer, W., Lima, M. G. and Medeiros-Junior, R. A. (2018) 'Fuzzy logic for estimating chloride

383 diffusion in concrete', *Proceedings of the Institution of Civil Engineers - Structures and Buildings*,

384 171(7), pp. 542–551. doi: 10.1680/jstbu.16.00153.

385 Miranda, J. M. *et al.* (2007) 'Limitations and advantages of electrochemical chloride removal in

386 corroded reinforced concrete structures', *Cement and Concrete Research*, 37(4), pp. 596–603. doi:

387 10.1016/j.cemconres.2007.01.005.

388 Muthulingam, S. and Rao, B. N. (2014) 'Non-uniform time-to-corrosion initiation in steel reinforced

389 concrete under chloride environment', *Corrosion Science*, 82, pp. 304–315. doi:

390 10.1016/j.corsci.2014.01.023.

391 Nguyen, T. H. Y. *et al.* (2021) 'Electrochemical chloride extraction on reinforced concrete

392 contaminated external chloride: Efficiencies of intermittent applications and impacts on hydration

393 products', *Cement and Concrete Composites*, 121, p. 104076. doi:

394 10.1016/j.cemconcomp.2021.104076.

395 Sánchez, M. and Alonso, M. C. (2011) 'Electrochemical chloride removal in reinforced concrete
396 structures: Improvement of effectiveness by simultaneous migration of calcium nitrite', *Construction
397 and Building Materials*, 25(2), pp. 873–878. doi: 10.1016/j.conbuildmat.2010.06.099.

398 Saraswathy, V., Lee, H.-S., *et al.* (2018) 'Extraction of chloride from chloride contaminated concrete
399 through electrochemical method using different anodes', *Construction and Building Materials*, 158, pp.
400 549–562. doi: 10.1016/j.conbuildmat.2017.10.052.

401 Saraswathy, V., Lee, H. S., *et al.* (2018) 'Extraction of chloride from chloride contaminated concrete
402 through electrochemical method using different anodes', *Construction and Building Materials*, 158, pp.
403 549–562. doi: 10.1016/j.conbuildmat.2017.10.052.

404 Shi, X. *et al.* (2012) 'Durability of steel reinforced concrete in chloride environments: An overview',
405 *Construction and Building Materials*, 30, pp. 125–138. doi: 10.1016/j.conbuildmat.2011.12.038.

406 Sun, G. *et al.* (2011) 'Multi-scale prediction of the effective chloride diffusion coefficient of concrete',
407 *Construction and Building Materials*, 25(10), pp. 3820–3831. doi: 10.1016/j.conbuildmat.2011.03.041.

408 Toumi, A., François, R. and Alvarado, O. (2007) 'Experimental and numerical study of
409 electrochemical chloride removal from brick and concrete specimens', *Cement and Concrete Research*,
410 37(1), pp. 54–62. doi: 10.1016/j.cemconres.2006.09.012.

411 Wang, Y., Gong, X. and Wu, L. (2019) 'Prediction model of chloride diffusion in concrete considering
412 the coupling effects of coarse aggregate and steel reinforcement exposed to marine tidal environment',
413 *Construction and Building Materials*, 216, pp. 40–57. doi: 10.1016/j.conbuildmat.2019.04.221.

414 Wang, Y., Li, L. Y. and Page, C. L. (2001) 'A two-dimensional model of electrochemical chloride
415 removal from concrete', *Computational Materials Science*, 20(2), pp. 196–212. doi: 10.1016/S0927-
416 0256(00)00177-4.

417 Wang, Yuanzhan *et al.* (2018) 'Prediction model of long-term chloride diffusion into plain concrete
418 considering the effect of the heterogeneity of materials exposed to marine tidal zone', *Construction and
419 Building Materials*, 159, pp. 297–315. doi: 10.1016/j.conbuildmat.2017.10.083.

420 Wu, L., Li, W. and Yu, X. (2017) 'Time-dependent chloride penetration in concrete in marine
421 environments', *Construction and Building Materials*, 152, pp. 406–413. doi:
422 10.1016/j.conbuildmat.2017.07.016.

423 Xia, J., Liu, Q., *et al.* (2018) 'Effect of environmental temperature on efficiency of electrochemical

424 chloride removal from concrete', *Construction and Building Materials*, 193, pp. 189–195. doi:
425 10.1016/j.conbuildmat.2018.10.187.

426 Xia, J., Liu, Q. feng, *et al.* (2018) 'Effect of environmental temperature on efficiency of
427 electrochemical chloride removal from concrete', *Construction and Building Materials*, 193, pp. 189–
428 195. doi: 10.1016/j.conbuildmat.2018.10.187.

429 Xia, J. *et al.* (2019) 'Numerical simulation of steel corrosion in chloride contaminated concrete',
430 *Construction and Building Materials*, 228, p. 116745. doi: 10.1016/j.conbuildmat.2019.116745.

431 Xia, J. *et al.* (2020) 'Effect of the stirrup on the transport of chloride ions during electrochemical
432 chloride removal in concrete structures', *Construction and Building Materials*, 250, p. 118898. doi:
433 10.1016/j.conbuildmat.2020.118898.

434 Xu, J. and Li, F. (2019a) 'Numerical analysis on efficiency of electrochemical chloride extraction of
435 one side anode in concrete', *Ocean Engineering*, 179(February 2017), pp. 38–50. doi:
436 10.1016/j.oceaneng.2019.03.018.

437 Xu, J. and Li, F. (2019b) 'Numerical analysis on efficiency of electrochemical chloride extraction of
438 one side anode in concrete', *Ocean Engineering*, 179, pp. 38–50. doi: 10.1016/j.oceaneng.2019.03.018.

439 Zhou, Y. *et al.* (2020) 'Reliability-based design analysis of FRP shear strengthened reinforced concrete
440 beams considering different FRP configurations', *Composite Structures*, 237, p. 111957. doi:
441 10.1016/j.compstruct.2020.111957.

442 Zhu, X. and Zi, G. (2017) 'A 2D mechano-chemical model for the simulation of reinforcement
443 corrosion and concrete damage', *Construction and Building Materials*, 137, pp. 330–344. doi:
444 10.1016/j.conbuildmat.2017.01.103.

445